Geometrical modelling and thermal analysis of nonwoven fabrics

Geometrical Modelling and Thermal Analysis of Nonwoven Fabrics

Muhammad Owais Raza Siddiqui [1, 2,*] Danmei Sun[2] and Ian B Butler[3]

[1]Department of Textile Engineering, NED University of Engineering and Technology, Karachi, 75270, Pakistan

[2]School of Textiles and Design, Heriot-Watt University, TD1 3HF, UK

[3]University of Edinburgh

[1]Corresponding author: **Muhammad Owais Raza Siddiqui**

E-mail address: orazas@neduet.edu.pk

Abstract

Nonwoven fabric can be produced for insulation. It has low fibre volume because insulation property of fibrous materials depends on not only the thermal conductivity of fibre but also the entrapped static air. If fibre volume fraction is low in fibrous assembly it means that more air in the volume therefore the insulation property of the fabric increases, or vice versa. In this research thermal bonded nonwoven fabrics were used to analyse the heat transfer phenomena and predict the effective thermal conductivity and thermal resistance by using finite element (FE) method. FE models of nonwoven fabrics were created by two techniques: 3D reconstruction and solid modelling. For validation purpose the effective thermal conductivity results obtained from an in-house developed instrument were compared with predicted results from the developed FE models. Furthermore, this research work also contains an investigation of the effect of fibre volume fraction and thermal conductivity of fibre on the overall heat transfer of nonwoven structures.

Keywords: Effective thermal conductivity, nonwoven fabric, finite element analysis, 3D reconstruction, image analysis

1 Introduction

Nonwoven fabrics are widely used in many application areas such as, insulation, filtration, health care, protective clothing, automotive interiors, consumer and industrial wipes because of their specific thermal property, filtering, bacterial barrier, flame -retardancy, resilience, stretch, softness, strength, and absorbency[1].

Many researchers have analysed the heat transfer through fibrous structures in terms of fibre conductance, bulk density and fibre arrangement. Bogaty et al. in 1957[2] studied the effect of pressure on thermal conductivity of fabric by using two plates method. They used the results of thermal conductivity of fabric obtained from the experimental device at different levels of pressure to find out the effective fraction of fibres parallel (x) and perpendicular (y) to the direction of heat flow by using Eq.1.

$$K_m = x\left(K_a V_a + K_f V_f\right) + y\left(\frac{K_a K_f}{K_a V_f + K_f V_a}\right) \qquad \text{Eq.1}$$

where K_a is the thermal conductivity of air, K_f is the thermal conductivity of fibre, V_a is the fractional volume of air, V_f is the fractional volume of fibre.

They concluded that:

1) thermal conductivity of fabric increases with the increase of proportion of fibres which are parallel to the heat flow at higher bulk density;
2) thermal resistance of fabric can be improved by using low thermal conductive fibres which are arranged parallel to the surface or perpendicular to the direction of heat flow; and
3) at a given bulk density the insulation property of fabric can be improved by using higher density of fibre because fibre volume fraction is dependent on the bulk and fibre density. The fact is that the fibre volume fraction is inversely proportional to fibre density. It means that the higher the fibre density at given bulk density the less the fibre volume fraction will be hence the more volume fraction of air.

In the above model there is no consideration of thermal anisotropy of fibres in fabric. Imakoma[3] developed a unit cell model, as shown in Fig. 1, to determine the effective thermal conductivity of fibrous insulation by considering the conduction heat transfer.

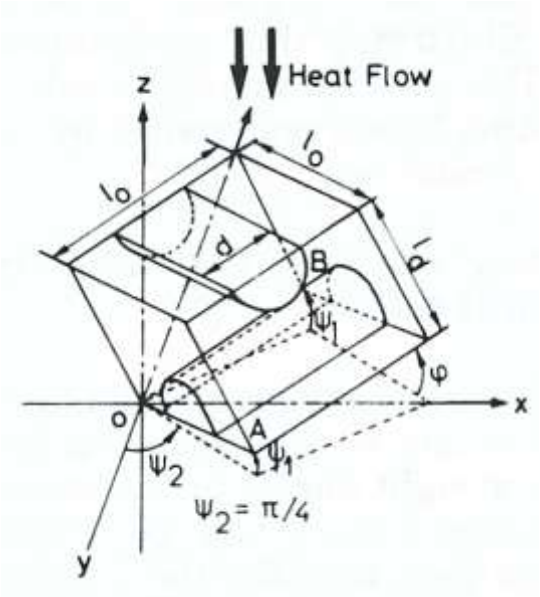

Fig. 1. Conduction heat transfer unit cell model [3].

Two semi cylinders represent two fibres which are parallel to the surface of the material. In this unit cell model there is no consideration of contact between fibres. In order to compensate this issue they proposed another unit

cell in which contact among the fibres was considered but it was assumed that the thermal resistance at contact point was much higher than that of within fibres. In their models random orientation of fibre was taken however they also failed to take into consideration of the thermal anisotropy nature of fibre. Naka and Kamata[4] analysed the thermal conductivity of wet fabric by varying the water content. In their model the effect of thermal anisotropy of fibre was considered in order to calculate the thermal conductivity of fabric normal (K_v) and parallel (K_w) to the surface by:

$$K_v = \frac{a}{2} K_{e\parallel} + \left(1 - \frac{a}{2}\right) K_{e\perp} \qquad \text{Eq.2}$$

$$K_w = d_w \left\{(1-a) K_{e\parallel} + a K_{e\perp}\right\} + d_f \left\{\frac{a}{2} K_{e\parallel} + \left(1 - \frac{a}{2}\right) K_{e\perp}\right\} \qquad \text{Eq.3}$$

where $K_{e\parallel}$ is the thermal conductivity of fibre parallel to the fibre axis, $K_{e\perp}$ is the thermal conductivity of fibre normal to the fibre axis, d_w is the thickness of warp layer, d_f is the thickness of weft layer and a is the ratio of fibres which are parallel and normal to the yarn.

In the above described model there was no consideration of actual orientation of fibre. Kawabata[5] evaluated the thermal anisotropy of fibre by measuring the thermal conductivity of fibre along and perpendicular to the fibre axis and the result of thermal conductivity of fibres obtained shows strongly in anisotropy. It is believed that in order to calculate the effective thermal conductivity of fibrous material it is necessary to consider the thermal anisotropy of fibre.

Kawabata measured the longitudinal thermal conductivity of fibres by clamping the parallel fibres in the copper chuck. The distance between the chucks/clamps or sample length is around 3~7 mm, sample width about 30 mm and cross-sectional area of fibres is about 3~5x10^{-6} m^2. Base chuck has constant flow of water and the temperature difference of 10°C was maintained by a built-in chuck sensor as shown in Fig. 2 (a). The longitudinal thermal conductivity (K_L) of fibre can be calculated by the Eq.4:

$$K_L = \frac{qL}{\Delta T A} \qquad \left(Jm^{-1}K^{-1}S^{-1}\right) \qquad \text{Eq.4}$$

where L is the length of the specimen (m), q is the heat flow *(JS^{-1})*, ΔT is the temperature difference (K) and A is the sum of the cross-sectional area of fibres (m^2).

In Kawabata's work the transverse thermal conductivity of fibre contained in composite plate was measured. The composite plate was composed of parallel fibre bundles which impregnated in epoxy at high pressure about 1 ton/cm^2 and cured. The thickness of plate is around 0.5-1 mm and the surface area of 5 x 5 cm^2 was placed between the plates as shown in Fig. 2 (b).

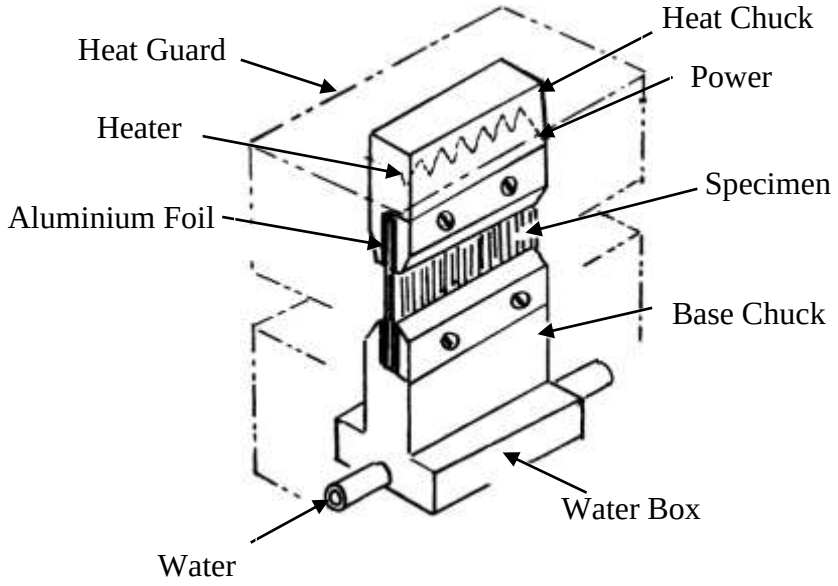

(a)

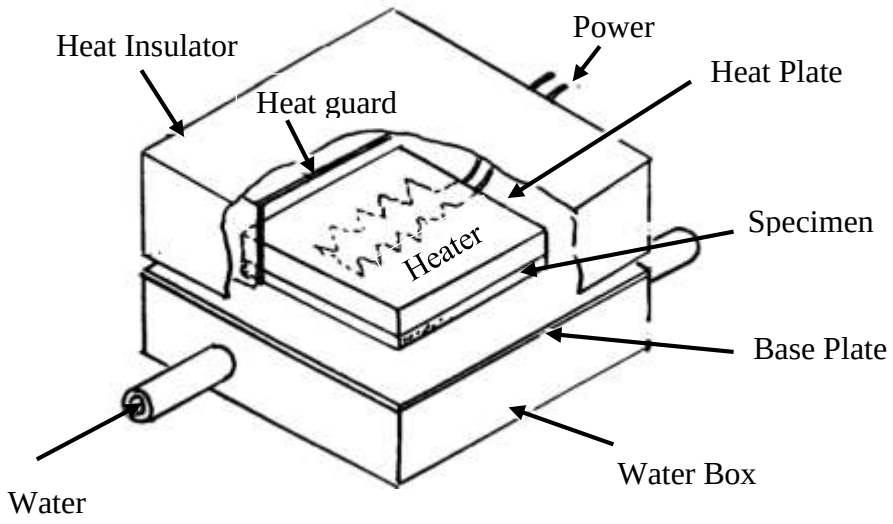

Fig. 2. Measuring head for measurement of thermal conductivity: (a) longitudinal and (b) transverse.

The transverse thermal conductivity of fibres was calculated by:

$$K_T = V_F \left(\frac{\Delta T \cdot A}{qL} - \frac{1 - V_F}{K_R} \right)^{-1} \qquad \text{Eq.5}$$

where V_F is the volume fraction of fibre, K_R is the thermal conductivity of resin, L is the plate thickness, A is the area of plate sample and ΔT is the temperature difference (10°C) .

Woo et al.[6] developed an analytical model for the thermal conductivity of nonwoven fabric in the transverse direction by considering fibre orientation, thermal anisotropy of fibre and fabric orthotropic effect as shown in Eq.6.

$$\begin{aligned} K_{oz} &= K_a \sin^2\phi P_i \\ &+ K_{\parallel} \cos^2\phi \alpha X_f / (1+\alpha) + \sin^2\phi (1-P_i)^2 \\ &\times \{1/[X_f / K_{|} + (1-P_i - X_f)/K_a]\} \\ &+ \cos^2\phi (1+\alpha-\alpha X_f)^2 / \{(1+\alpha)[X_f / K_{|} + (1+\alpha)/K_a]\} \end{aligned} \qquad \text{Eq.6 (a)}$$

and

$$P_i = \left[1-(8/\pi)X_f + (8/\pi)^2 X_f{}^2 \alpha/(1+\alpha)^2\right]^{L/(2d)} \qquad \text{Eq.6 (b)}$$

where K_{oz} is the thermal conductivity through the fabric, K_a is the thermal conductivity of air, $K_{|}$ and $K_{\parallel}$ are the thermal conductivities of the fibres along and across their axes respectively, X_f is the fibre volume fraction, α is the anisotropy factor, $\cos^2\phi$ is the polar orientation parameter, L is the fabric thickness, and d is the fibre diameter.

They analysed the effect of fabric geometry on thermal conductivity of the nonwoven fabric and concluded:

1) the conduction is the prominent mode of heat transfer, there is no evidence of convective heat transfer and radiative transfer was only effective when the fibre volume fraction is less than 3%;
2) the thermal conductivity of fabric is affected by the fibre volume fraction; and
3) the thermal conductivity of fabric is influenced by fibre orientation and thermal anisotropy of fibre. The overall thermal conductivity of the nonwoven fabric would increase for fibres arranged parallel to heat flow compared to that of the fibres arranged perpendicular to heat flow.

Nonwoven fabrics can be produced in three stages: web formation, web bonding and finishing (optional) as shown in Fig. **3**.

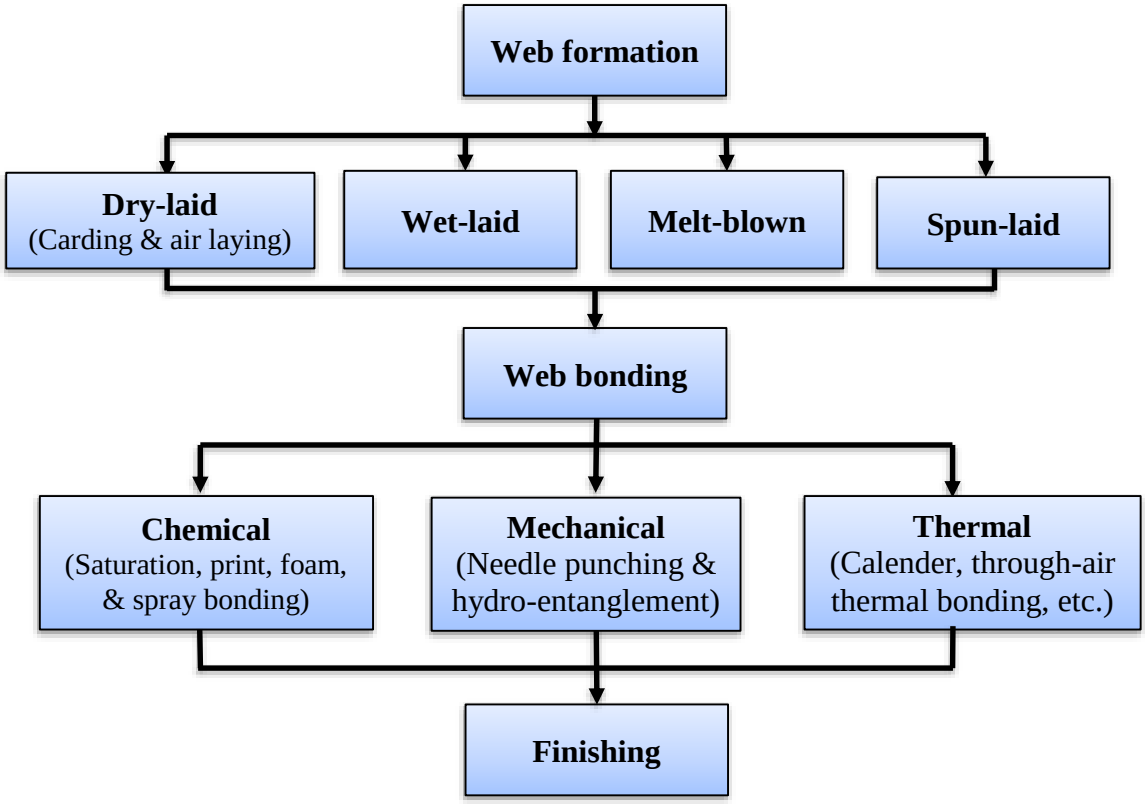

Fig. 3. Stages of nonwoven fabric manufacturing process

Fig. **4** shows the process flow of thermal point bonding of nonwoven fabric. Two rollers one smooth and other engraved are used. A web which contains thermoplastic fibre is passed through these two heated rollers; the web melts at the contact points and binds thermoplastic fibres to form a nonwoven fabric. The fabrics produced by this method are relatively softer than the fabric produced by thermal bonding with high pressure.

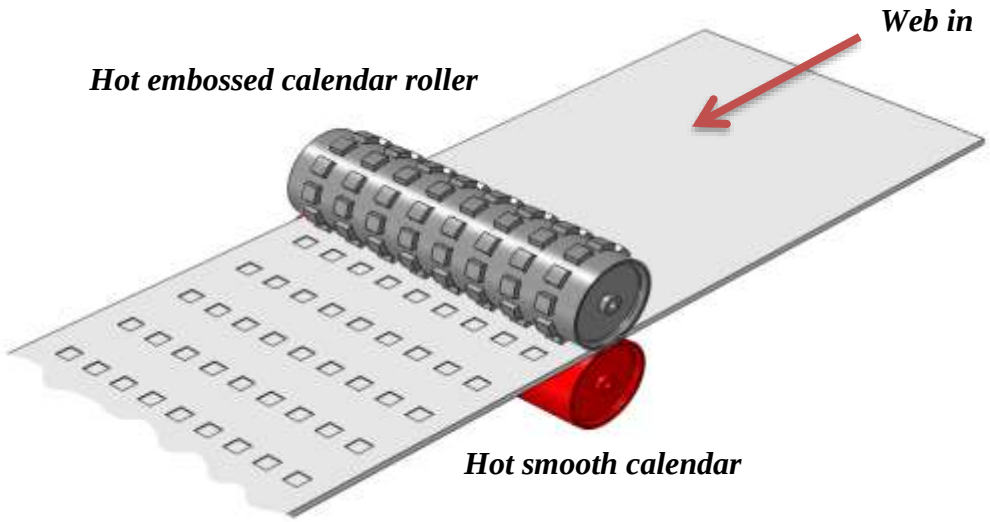

Fig. 4. Thermal point bonding process of nonwoven fabrics

The advantages of thermal bonding over other bonding techniques are:

1) energy efficient compared to chemical bonding because in chemical bonding high amount of energy is required to evaporate water from adhesive [7];
2) high production rate compared to chemical bonding [7];
3) environmental friendly because there is no any chemical involved; and
4) the end product developed have soft handle.

Thermal bonded nonwoven fabrics with unique structural properties and applications were used in this study. They have been used for protective clothing, cloth interlining, insulation etc. The heat transfer behaviour of thermally bounded nonwoven fabrics has not been studied by numerical analysis except randomly distributed nonwoven fabric[8-12]. In this study methods have been developed to predict the effective thermal conductivity of thermally bonded nonwoven fabric via finite element method by using the actual geometrical parameters of nonwoven fabric, analyse the fibre orientation by using 2D Fast Fourier Transform (FFT) and the effect of fibre volume fraction and thermal conductivity of fibre on the overall heat transfer of nonwoven structures. This will contribute to the knowledge base of nonwoven textile research and will be useful for nonwoven textile industry due to the rapid market growth of nonwoven fabrics and their applications[13].

2 Methodology

The following methodology is adopted to calculate the effective thermal conductivity and thermal resistance of thermal bonded nonwoven fabrics:

1) 3D reconstruction of thermally bonded nonwoven fabric by using µCT image;
2) unit cell modelling of nonwoven fabric by using repeating unit cell;
3) calculation of the effective thermal conductivity and thermal resistance of thermally bonded nonwoven fabric and analysis of the effect of thermal anisotropy and orientation of fibre using FE method; and
4) estimation of fibre orientation by using 2D Fast Fourier Transform (FFT).

2.1 Materials

In this study thermally bonded nonwoven fabrics made of polypropylene fibre (PP) were used. The fabric specifications and fibre properties are shown in Table I and Table II respectively.

Table I: Fabric specifications

Specifications	Sample-1	Sample-2	Sample-3
Areal density (g/m^2)	78.133	38.265	77.280
Thickness* (mm)	0.54	0.35	0.57
Fibre Material	polypropylene	polypropylene	polypropylene

* from µCT image

Table II: Fibre properties [14]

Property	Symbol	Values
Fibre density (Kg/m^3)	ρ	910
Axial fibre thermal conductivity (W/m.K)	K_{fa}	1.241
Transverse fibre thermal conductivity (W/m.K)	K_{ft}	0.111
Anisotropy	K_{fa}/K_{ft}	11.18
Fibre specific heat (J/Kg.K)	C_{pf}	1680

2.2 3D Reconstruction of Nonwoven Fabric

Nonwoven fabrics have complex and irregular structures as compared to woven and knitted fabrics. In this work the geometrical models of nonwoven fabrics were obtained by 3D reconstruction through High-resolution X-ray Computer Tomography (CT). In X-ray CT the samples are rotated around a vertical axis in front of X-ray source and the reconstructed data come as slices and cut to normal to that axis, illustrated in Fig. 5 .

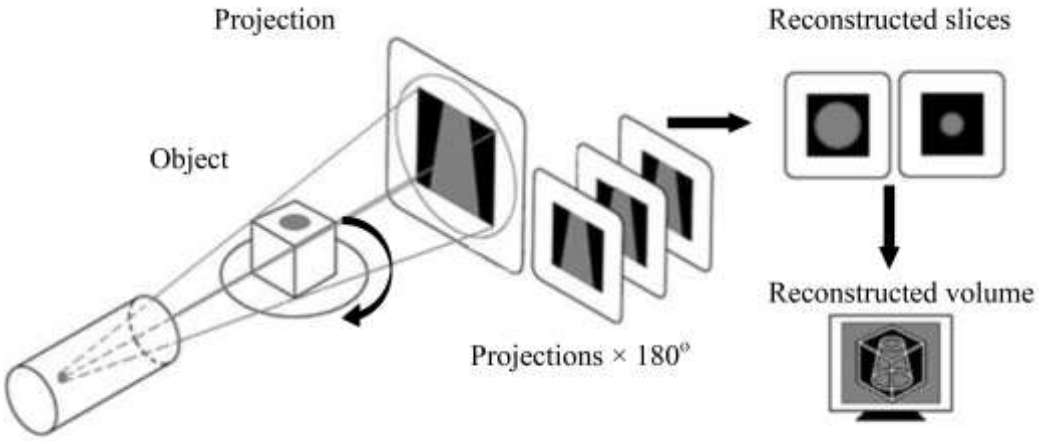

Fig. 5. Schematic of X-ray Tomography[15].

In order to develop the 3D reconstructed nonwoven fabrics, the fabric samples were cut in small strips with a scalpel and placed in boron nitride cup to hold (BN is extremely low in density and almost x-ray transparent).

A small angle cone X-ray beam source is used and samples are rotated around the vertical axis. Images are generated on the basis of X-ray attenuation showing the density of nonwoven fabric samples. These projection images are used to generate 2D slices which reflect the inside of the samples when it's cut to normal to the axis of rotation. The resolution of the data collected was 3.713 microns per voxel (a voxel is the volume equivalent to a pixel). Fig. 6 shows the 3D rendering of grey scale image achieved by ImageVis3D[16].

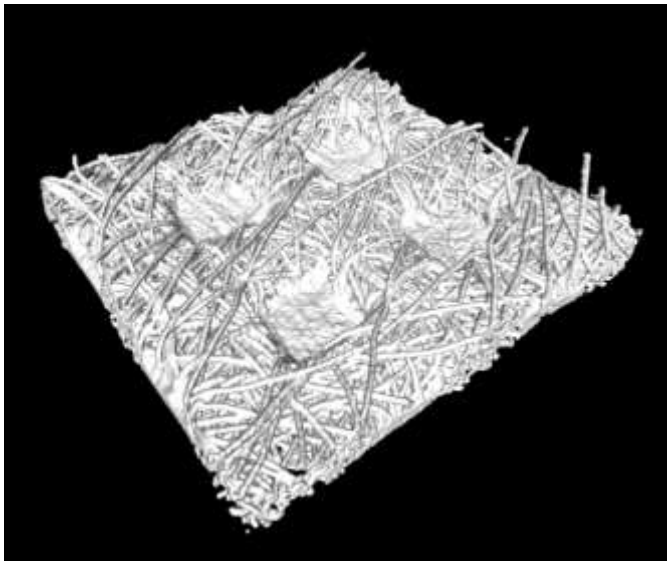

(a)

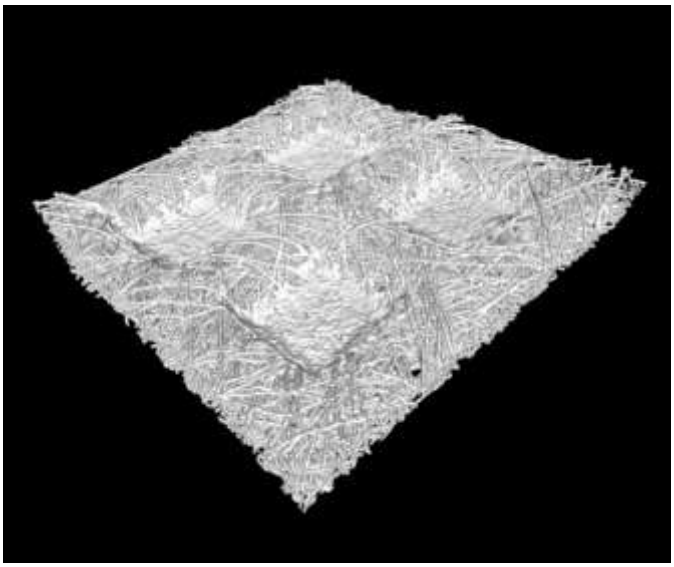

(b)

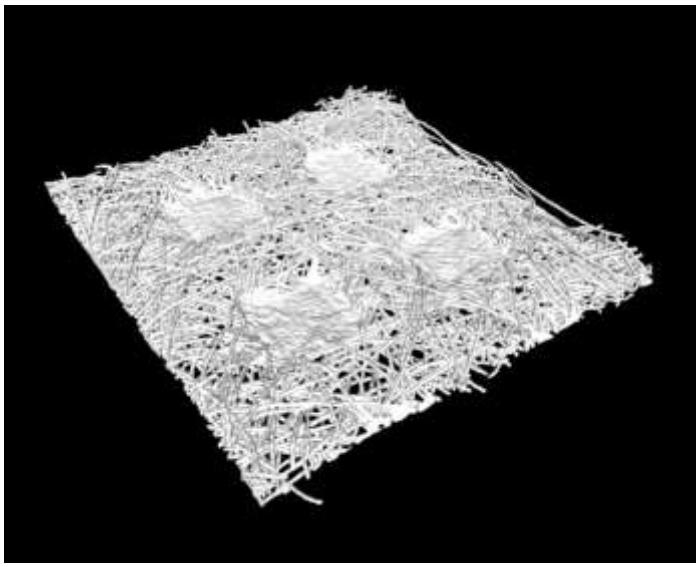

(c)

Fig. 6. 3D Rendering of: (a) sample-1; (b) sample-2; and (c) sample-3.

2.2.1 Unit Cell Model of Thermally Bonded Nonwoven Fabric

The unit cell models of thermally bonded nonwoven fabrics have been developed by using repeat unit cell approach, shown in Fig. 7. The following two techniques were used:

1) X-ray Computer Tomography (CT); and
2) solid model generation by using 3D reconstructed STL (Stereolithography/Standard Tessellation Language) mesh model.

2.2.1.1 Unit Cell Model from X-ray Computer Tomography (CT)

Unit cell model of thermally bonded nonwoven fabrics obtained from the X-ray Computer Tomography (CT) were created in four steps:

1) image collection, 2D slice reconstruction and segmentation;
2) 3D reconstruction and STL surface mesh generation;
3) restoration and simplification of STL surface mesh; and
4) solid unit cell model formation of STL surface mesh.

2.2.1.1.1 Image Collection, 2D Slice Reconstruction and Segmentation

1429 2D grey scale sliced images obtained from CT scan were assembled in ImageJ [17] to develop the stack. These stack images were binarised/segmented in order to extract the solid fibrous portion from their backgrounds by using sufficient thresholds of grey levels. In this work Otsu algorithm [18] was utilized to binarise the stack of images as shown in Fig. 8. Otsu algorithm binarises the image by the following steps:

1) calculate the grey level of normalized histogram of the input image;
2) find the potential threshold level of input image and categorize the pixel into two groups (background and foreground);
3) calculate the mean of each group;
4) calculate the between-class variance (σ_B^2);
5) obtain the optimal threshold that maximises the between-class variance (σ_B^2) or minimises the weighted within class variance; and
6) use the optimal threshold to binarise the input image.

The drawback of Otsu's method is that it fails in case of the object and background pixels are extremely unstable (unimodality of the object function). During the segmentation of the stack images in ImageJ by using Otsu's

method it is important to use the optimum threshold level to ensure that the fibre volume fraction of thermally bonded nonwoven fabric will not be changed. If the fibre volume fraction is changed during the segmentation process, the effective thermal conductivity will be affected significantly.

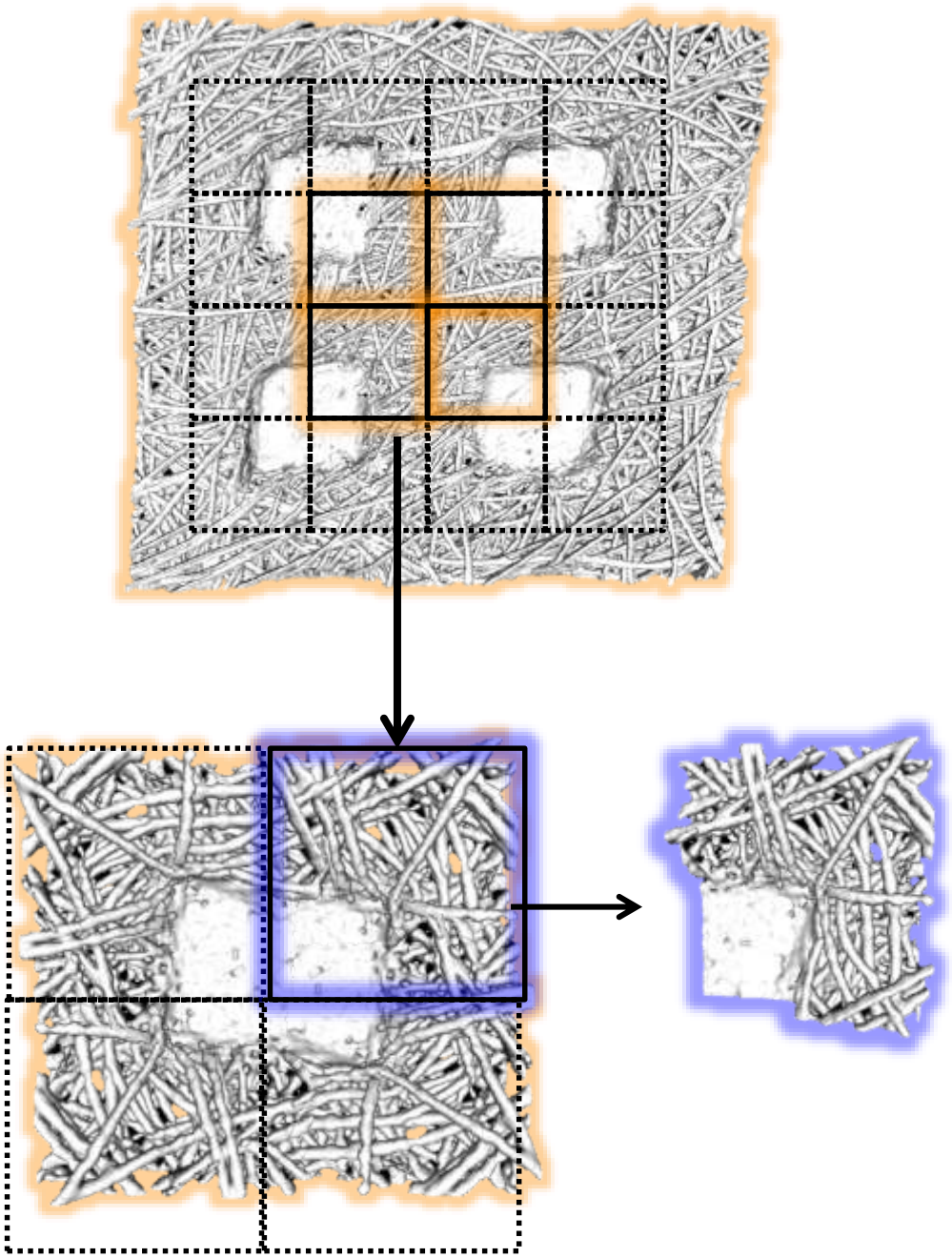

Fig. 7. Unit cell model of thermally bonded nonwoven fabric.

2.2.1.1.2 3D reconstruction and STL Surface Mesh Generation

After the segmentation step, stack images were cropped and the slices were reduced in order to obtain the quarter unit cell of thermally bonded nonwoven fabric. A 3D viewer plugin [19] of ImageJ was used to generate surface

mesh (shell) of sample-1 in STL format which contains 254388 triangular faces, 381582 edges and 126778 vertices.

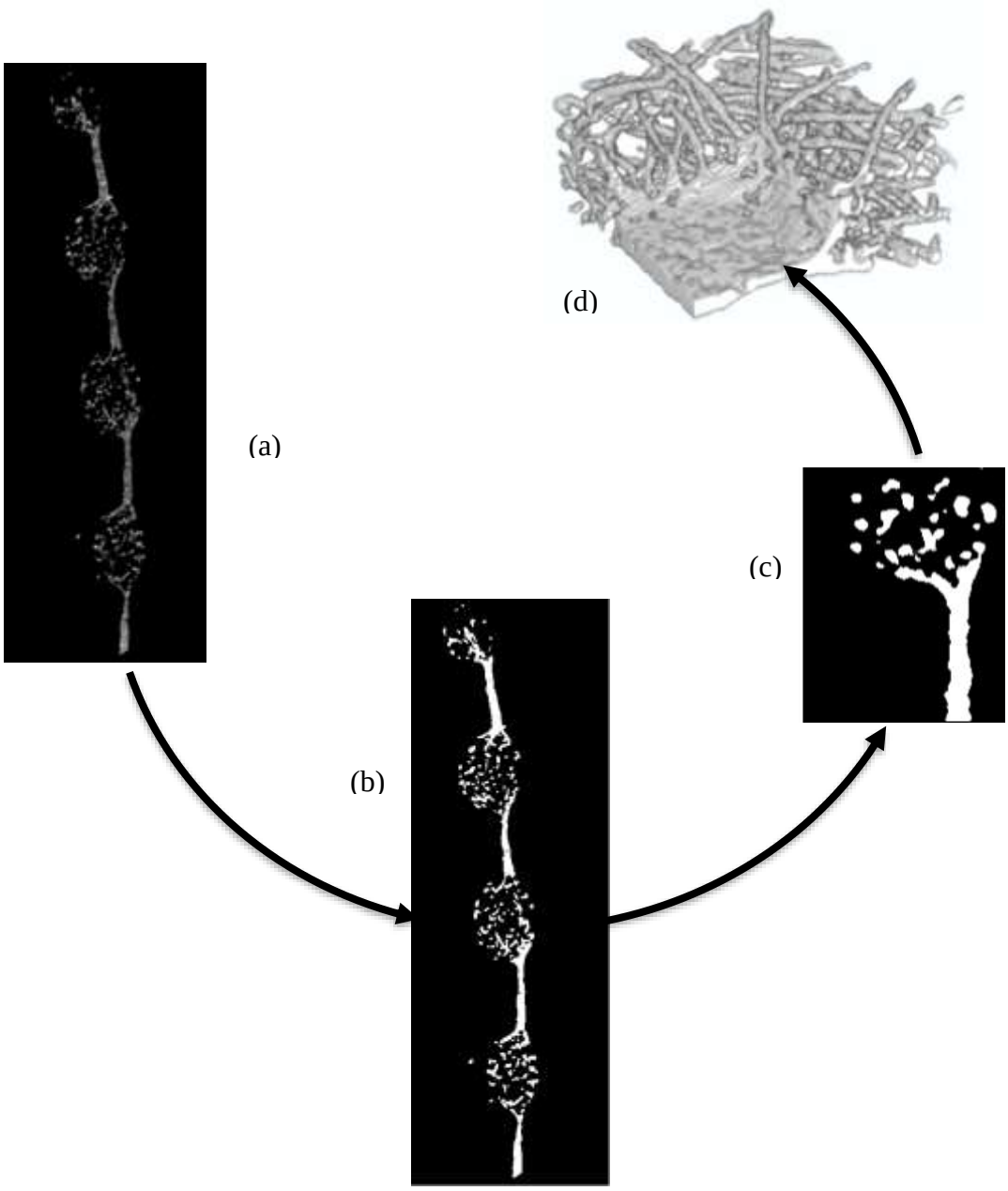

Fig. 8. 3D reconstruction steps (a) 2D grey scale stack slice image of sample-1; (b) segmented image by Otsu's method; (c) cropped unit cell segmented image of sample-1; and (d) 3D reconstructed unit cell of sample-1.

2.2.1.1.3 Restoring and Simplification of STL Surface Mesh

Surface mesh file was imported in MesLab [20] and filters were applied to remove the duplicate faces, zero area faces and self-intersecting faces. Quadratic edge collapse decimation was also used to reduce the number of faces which ultimately reduced the computing cost and time. Fig. **9** shows how this Quadratic edge collapse decimation filter works. When quadratic edge collapse decimation filter is applied it is important to make sure that the

geometric parameter mesh volume keeps no change because it represents the fibre volume fraction. After applying Quadratic edge collapse decimation filter the faces of sample-1 reduced from 254388 to 40000.

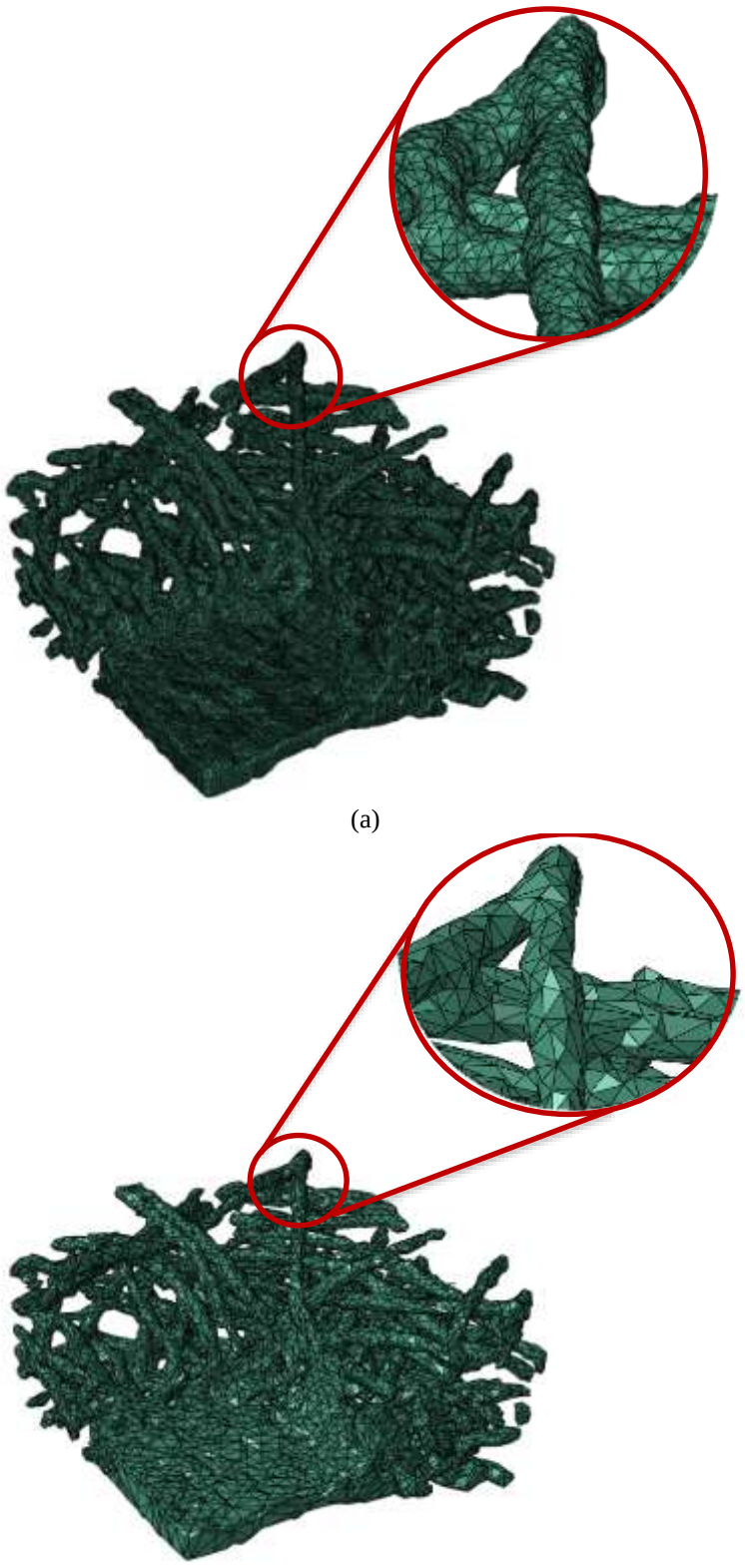

(a)

(b)

Fig. 9. Faces reduction: (a) sample-1 with 254388 faces and (b) sample-1 with 4000 faces after Quadratic edge collapse decimation filter

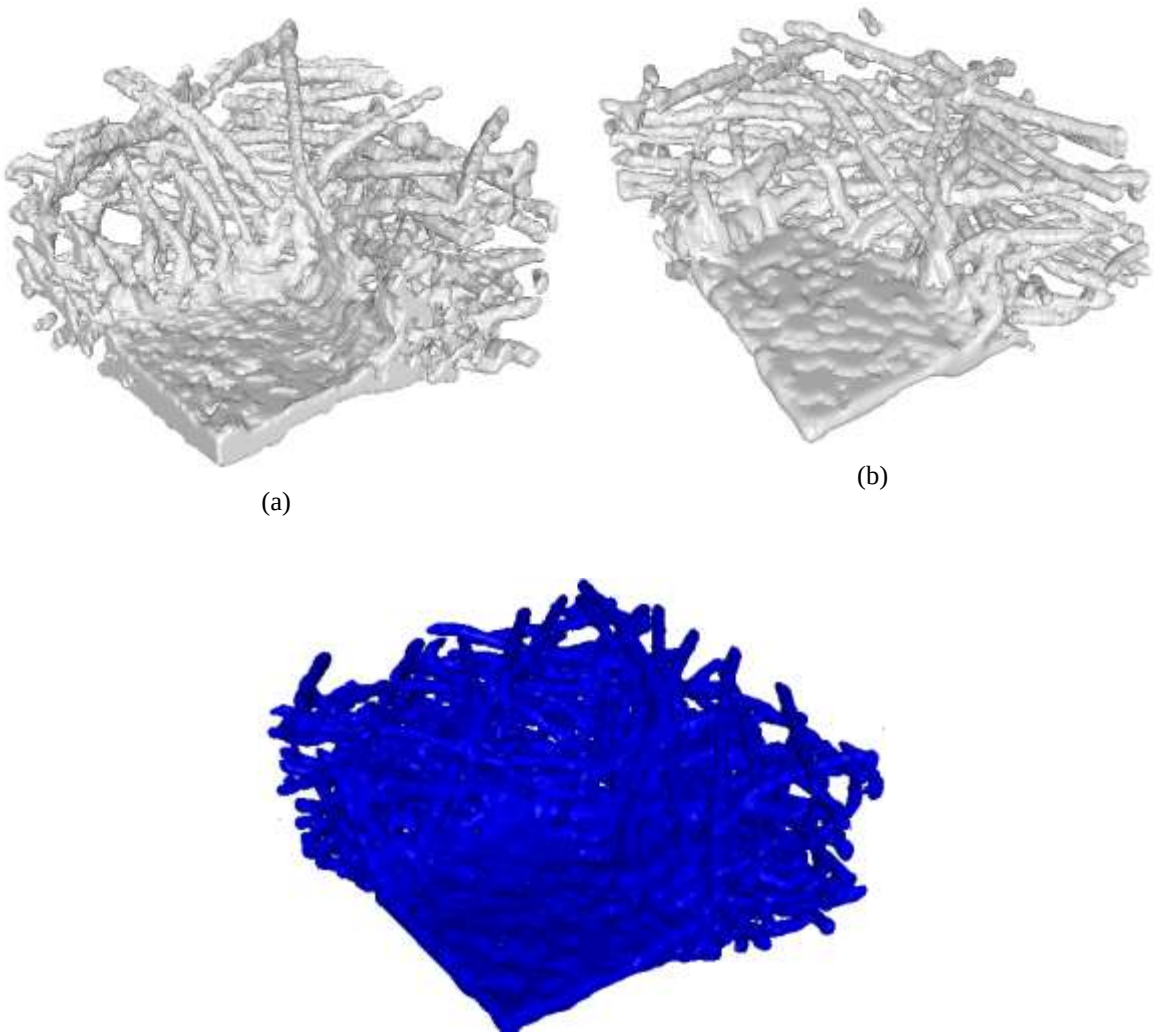

(a) (b) (c)

Fig. 10. STL mesh model: (a) sample-1; (b) Sample-2; and (c) sample-3.

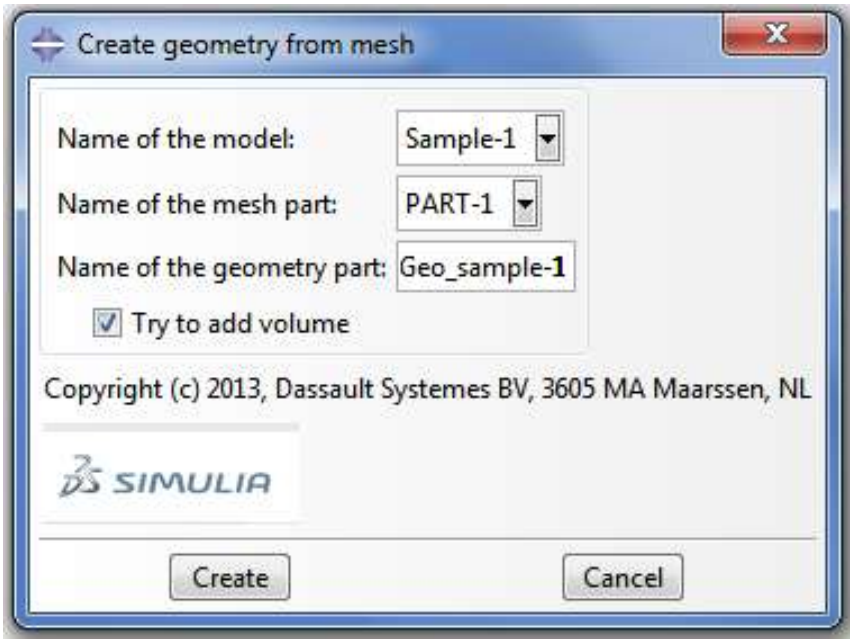

Fig. 11. Create geometry from mesh plug-in.

2.2.1.2 Unit Cell Model by Using 3D Reconstructed STL Mesh Model

Solid unit cell model was developed by using STL mesh model as shown in Fig. 12. The parametric dimensions of thermally bonded nonwoven fabrics were determined in MeshLab by using STL mesh models and described in Table **III**. It is assumed that the bond points were solid without any porosity, while the fibrous part is considered as solid, shown in Fig. 12 (b). Their fibre volume fraction values need to be calculated.

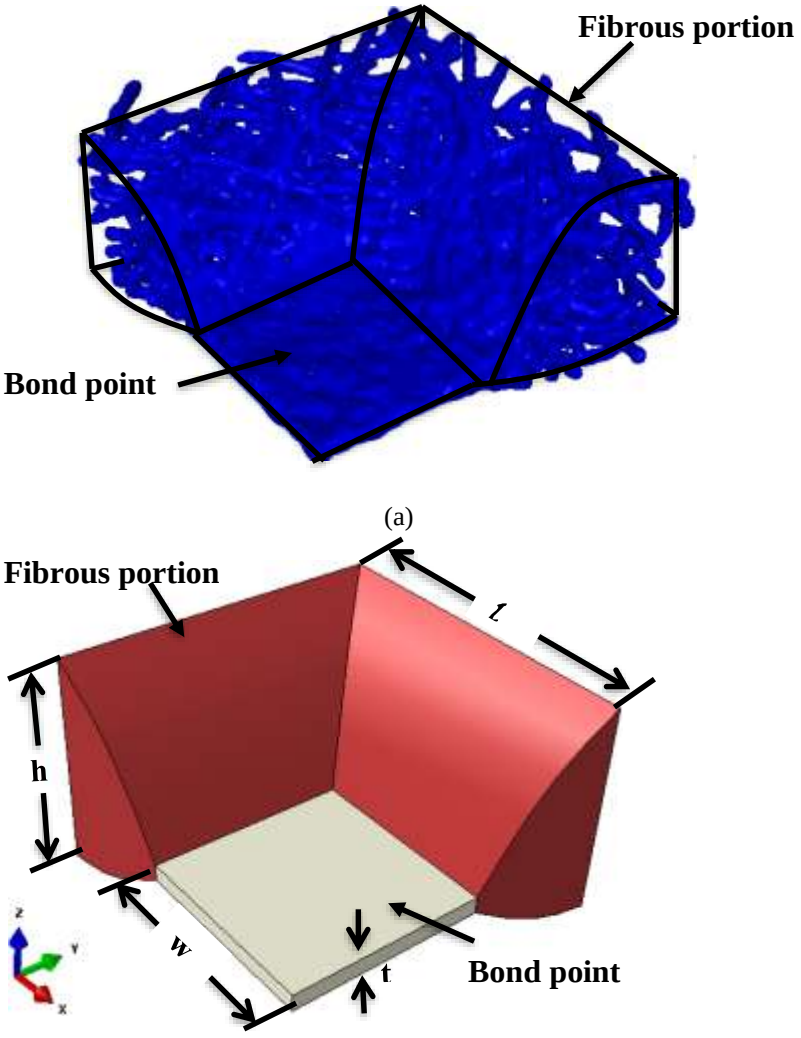

Fig. 12. Nonwoven models: (a) STL mesh model of sample-3 and (b) Solid model of sample-3.

Fibre volume fraction of fibrous portion (V_{fp}) can be determined by the total mesh volume in the following steps:

1) calculate the volume of bond point (v_{BP});
2) calculate the fibrous portion volume (v_{FP}) by subtracting the volume of bond point from the total mesh volume (v_M); and
3) calculate the volume fraction of fibrous part in solid model by Eq.7.

$$V_{fp} = \frac{v_{FP}}{v_{SF}} \qquad \text{Eq.7}$$

where v_{SF} is the total volume of fibrous portion as solid in solid model.

Table III. Sample geometric dimensions

Samples	h (mm)	l (mm)	w (mm)	t (mm)	v_{SF} (mm^3)
Sample-1	0.54	0.720	0.3560	0.0550	0.150
Sample-2	0.35	0.787	0.4185	0.0322	0.104
Sample-3	0.57	0.904	0.5130	0.0430	0.213

3 Effective Thermal Conductivity of Thermally Bonded Nonwoven Fabric

Effective thermal conductivity of thermally bonded nonwoven fabric was determined with consideration of the following assumptions:

1) there is no compression in nonwoven fabric when it is placed between the two plates during thermal conductivity testing; and
2) entrapped air between the two plates and within in the fibrous portion of the nonwoven fabrics is considered as fluid matrix, shown in Fig. 13.

3D reconstructed and solid model with air fluid is shown in Fig. 14. Thermal conductivity value of fibrous portion (K_{fp}) in solid nonwoven fabric model was calculated by:

$$K_{fp} = \frac{K_{ft} K_{air}}{V_{fp} K_{air} + (1 - V_{fp}) K_{ft}} \quad \text{Eq.8}$$

Table IV shows the fibre volume fraction of thermally bonded nonwoven fabrics. The thermal conductivity of their fibrous portion will be used as input material property in Abaqus/CAE. Only transverse thermal conductivity of fibre was considered because it is very difficult to assign the material orientation to provide anisotropic values of thermal conductivity. Sample-1 was 3D reconstructed and all solid models were meshed by 4-node linear tetrahedral elements (DC3D4). The unit cell was analysed by one dimensional steady state transfer analysis with applied temperature specified boundary conditions and the effective thermal conductivity was calculated by the Fourier's law of conduction:

$$Q_{cond} = -K_e A \frac{\Delta T}{t} \quad \text{Eq.9}$$

where K_e, A, ΔT and t are the effective thermal conductivity, surface area, temperature gradient and thickness of thermally bonded nonwoven unit cell respectively.

Table V shows he predicted effective thermal conductivity and thermal resistance by FE analysis. Fig. 15 and Figs. 16-18 show the heat flux and temperature contour of 3D reconstructed model and solid model respectively.

Table IV: Fibre volume fraction and thermal conductivity of nonwoven fabric

Samples	Fibre Volume Fraction of unit cell, V_f (%)	Fibre volume fraction of fibrous portion, V_{fp} (%)	Thermal Conductivity of fibrous portion, K_{fp} * (W/m.K)
Sample-1	15.95	25.112	0.03219
Sample-2	12.01	19.59	0.03059
Sample-3	14.93	27.42	0.032911

* K_{fp} calculated on the bases of transverse thermal conductivity of fibre

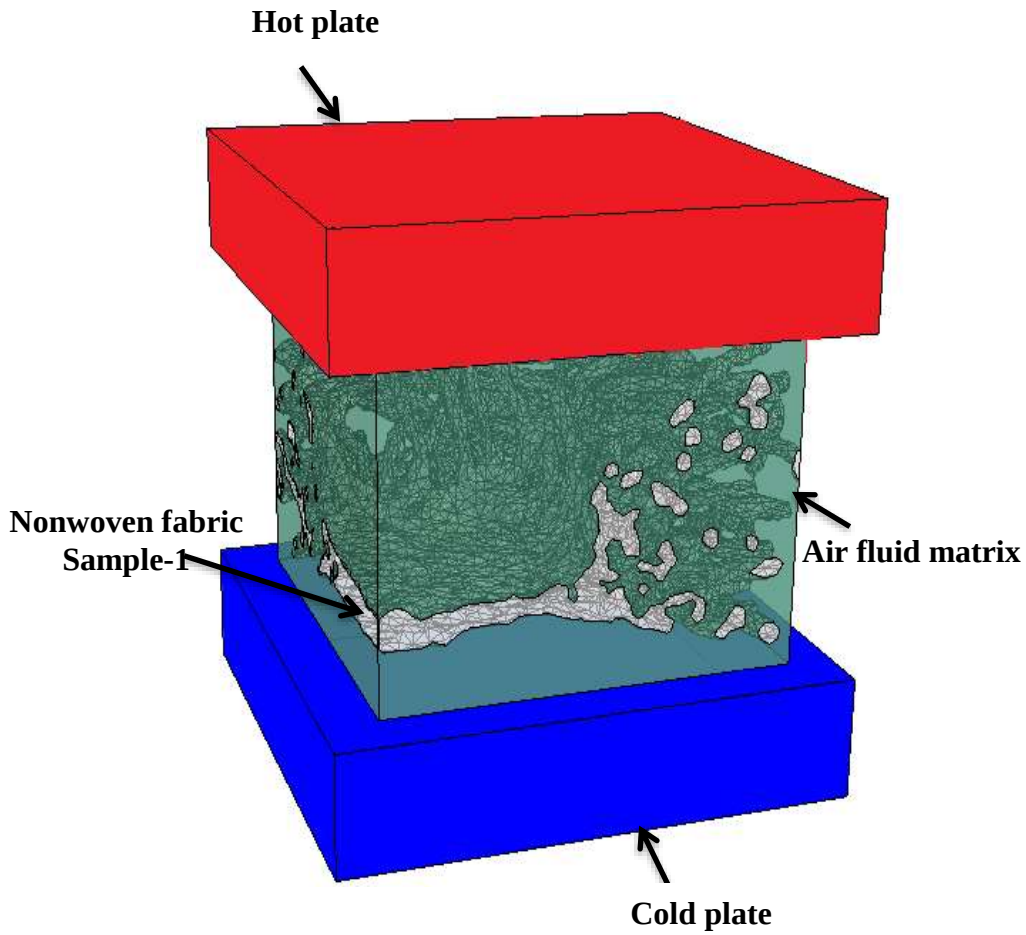

Fig. 13. Experimental and simulation setup.

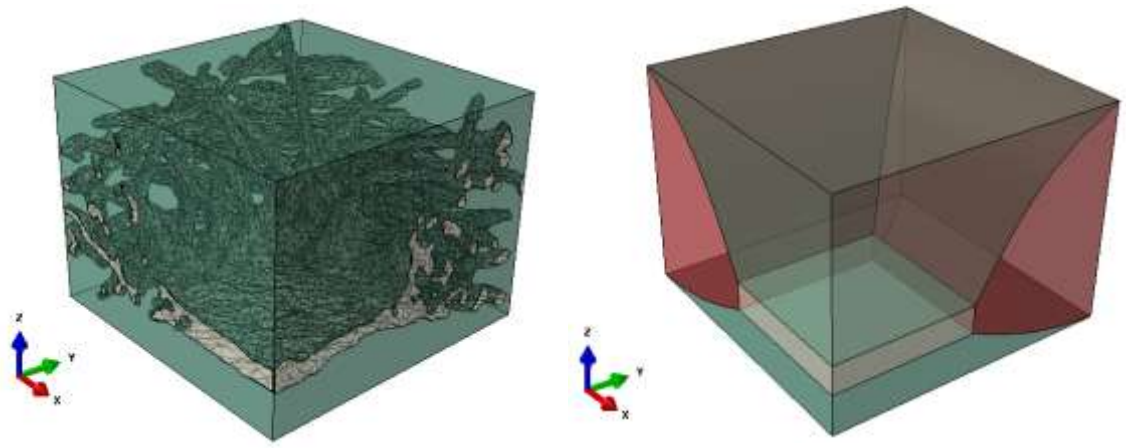

(a) (b)

Fig. 14. Unit cell model of sample-1 with air fluid matric: (a) 3D reconstructed model and (b) solid model.

Table **V:** Predicted effective thermal conductivity and thermal resistance

Samples	Effective thermal conductivity (W/m.K)		Thermal Resistance (m^2.K/W)	
	3D reconstructed model	Solid model	3D reconstructed model	Solid model
Sample-1	0.03368	0.02981	0.01603	0.018115
Sample-2	-	0.02956	-	0.01184
Sample-3	-	0.02873	-	0.01984

Figs.16 to 18 shows the heat flux contour of solid unit cell model of thermally bonded nonwoven fabrics. The fibrous portion has less thermal conductivity as compared to the solid bond point, as a result, the contact point between the solid fibrous portion and bond point makes the heat flux profile changed. This effect is especially significant for sample-1as it has thicker bond point as compared to the other two samples.

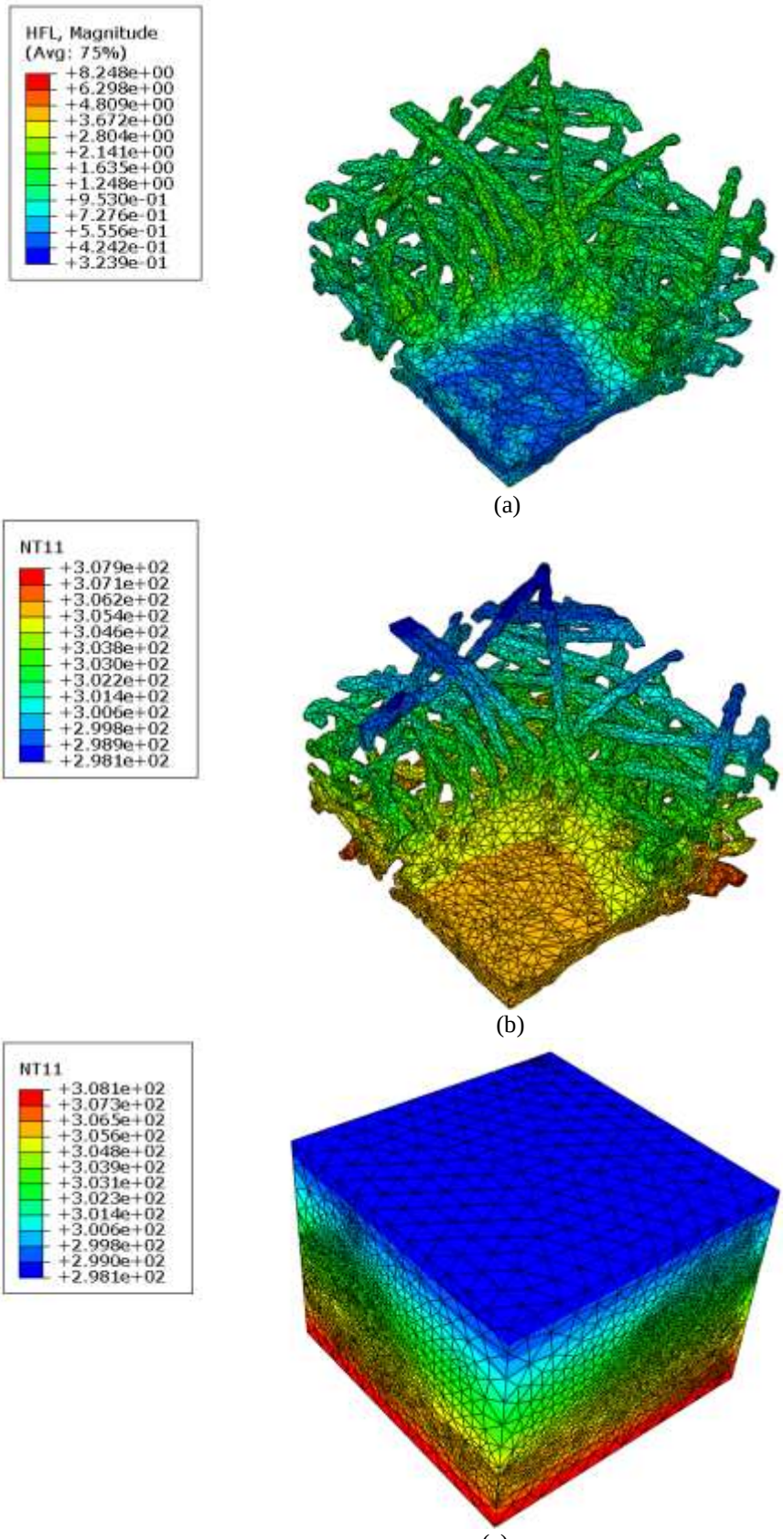

Fig. 15. Unit cell model of sample-1 with air fluid matric: (a) Heat flux Contour of sample-1; (b) Temperature contours of sample-1; and (c) temperature contours of sample-1 with air fluid matrix.

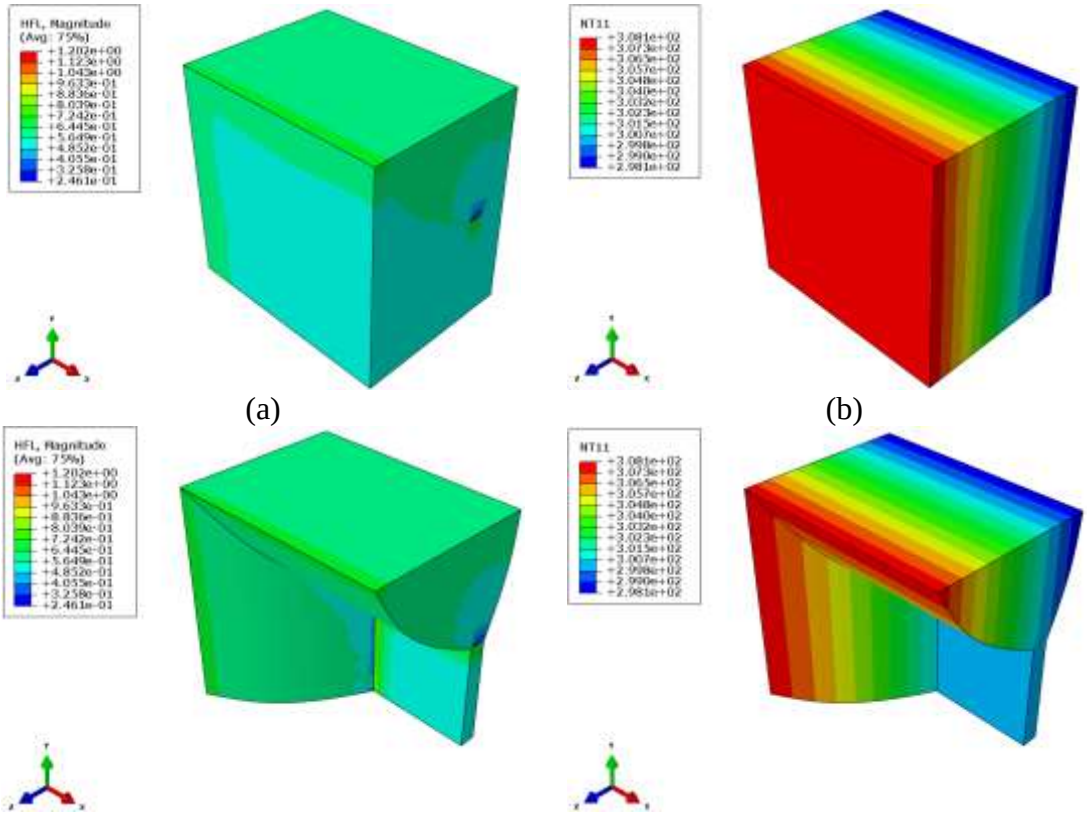

Fig. 16. Heat flux and temperature contour of unit cell model of sample-1 (a & b) with air fluid matrix and (c & d) without air fluid matrix.

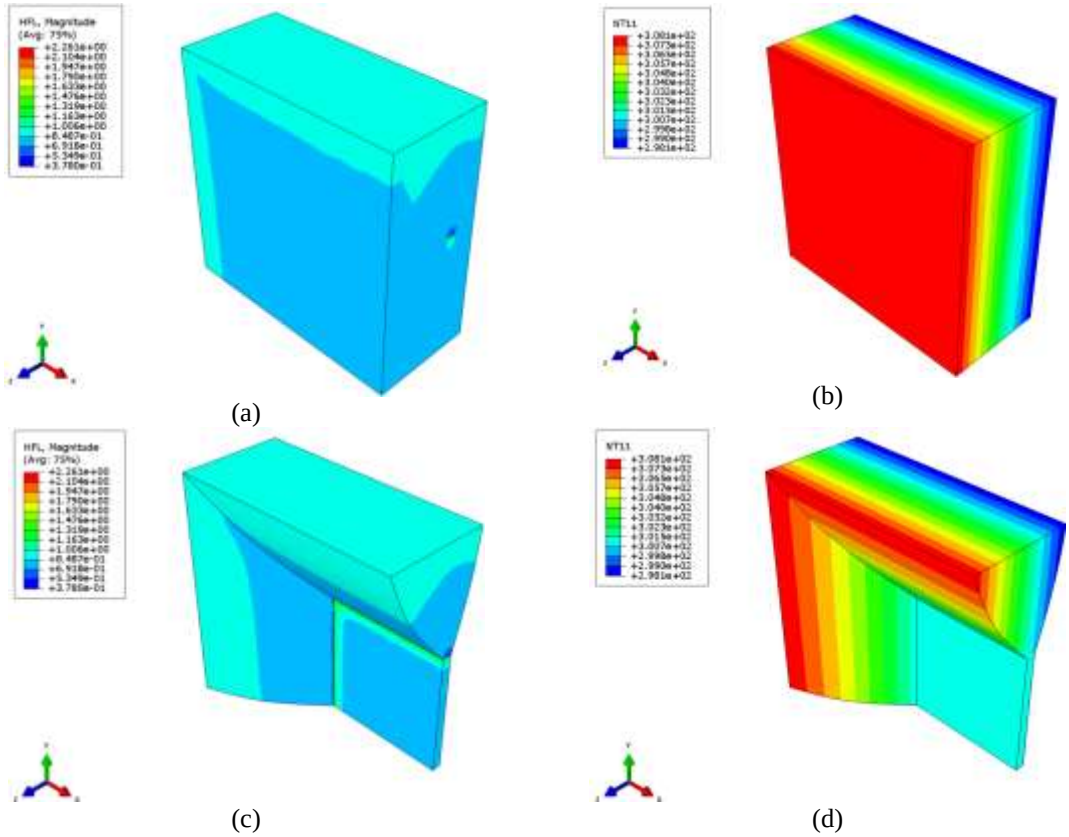

Fig. 17. Heat flux and temperature contour of unit cell model of sample-2 (a & b) with air fluid matrix and (c & d) without air fluid matrix.

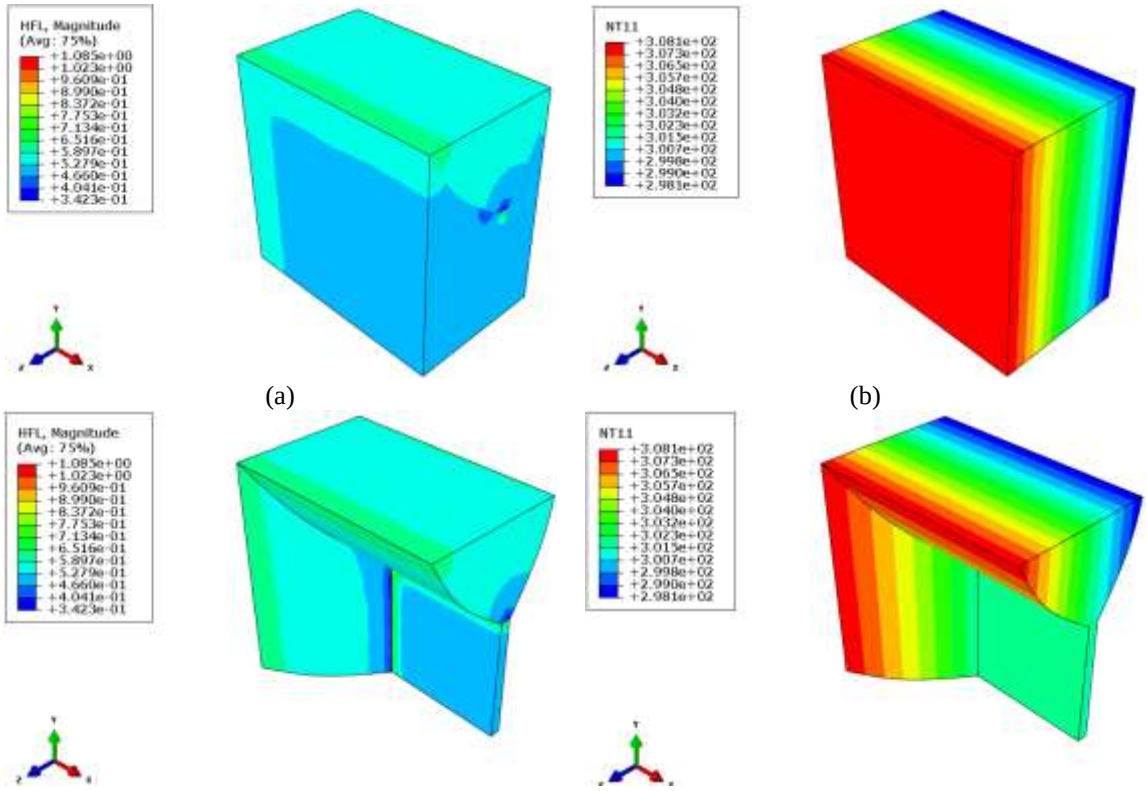

Fig. 18. Heat flux and temperature contour of unit cell model of sample-3 (a & b) with air fluid matrix and (c & d) without air fluid matrix.

3.1 Experiment and Model Validation

In order to validate the model of thermally bonded nonwoven fabric comparison has been made between the experimental results and predicted results by FE analysis. The three nonwoven fabrics were tested by using an in-house developed instrument and the tested results are shown in Table VI. The detailed information about the instrument and testing technique can be found in reference [21].

Table VI: Experimental results

Samples	Effective thermal conductivity (W/m.K)	Thermal resistance (m^2.K/W)
Sample-1	0.037335	0.014464
Sample-2	0.036146	0.009683
Sample-3	0.033889	0.01682

Fig. 19 shows the comparison between the experimental and predicted results of thermal conductivity. It shows good linear relationship between the two reflected by high correlation factor of 0.992372 and coefficient of determination of 0.98. However there is high absolute mean error (17.86638%) between the experimental and predicted results, this can be explained by the fact that there was no consideration of fibre orientation and thermal

anisotropy of fibres in the nonwoven fabric. This is agreed well with the finding in reference[21], that the isotropic analysis has more error as compared to the anisotropic conditions.

Fig. 20 shows the comparison between the experimental and predicted results of thermal resistance. It shows good linear relationship between the two reflected by correlation factor of 0.992378 and coefficient of determination of 0.9848. However there is high absolute mean error (21.8267%) between the experimental and predicted results, caused by the same reason explained above.

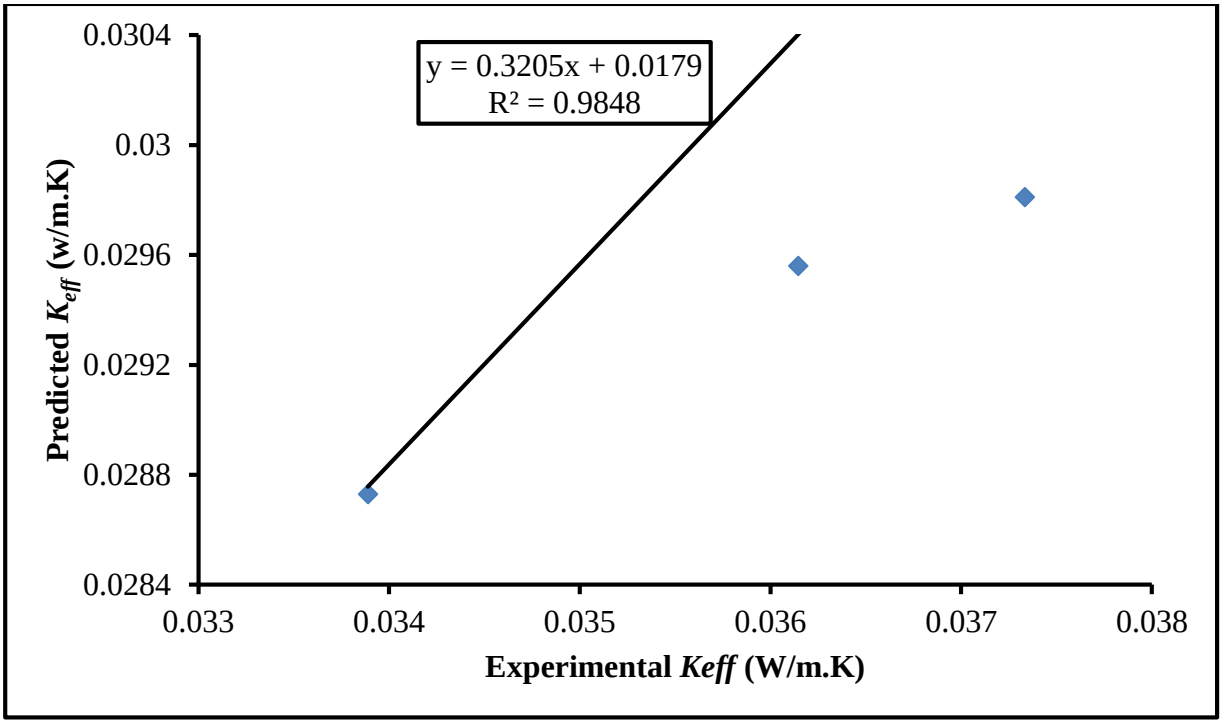

Fig. 19. A Comparison of effective thermal conductivity between predicted by FE model and experiment.

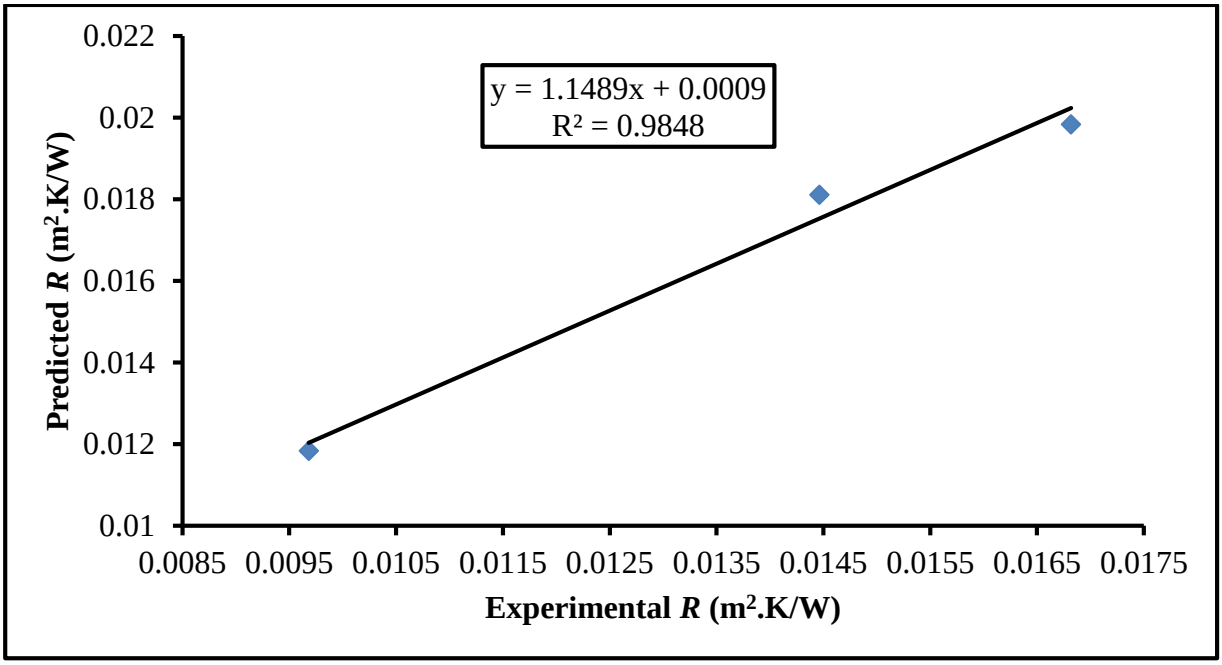

Fig. 20. A Comparison of thermal resistance between predicted by FE model and experiment.

The next step is to evaluate the orientation of nonwoven fabric. For this purpose 2D Fast Fourier Transform (FFT) was utilized to measure the alignment fibres in nonwoven fabric. A 2D SEM image was utilized and a cropped portion between the two bonding points was taken for analysis of fibre orientation, presented in Fig. 21.

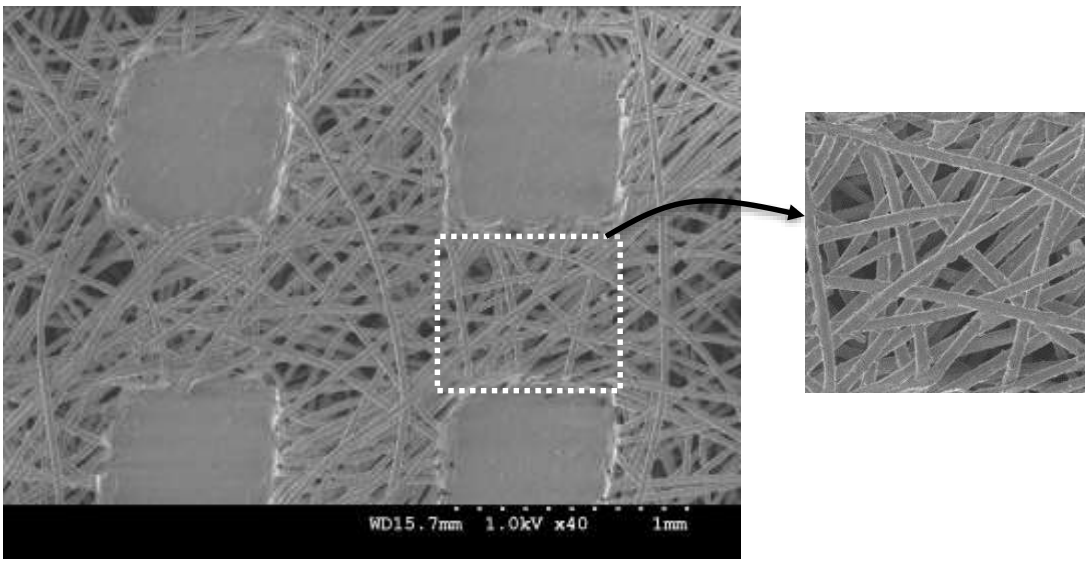

Fig. 21. Micrograph of sample-1.

Fibre orientation of thermally bonded nonwoven fabric has been evaluated by the following steps described by Ayres et al. [22]:

1) 2D-FFT was performed on grey scale image of thermally bonded nonwoven fabric. Only when the cropped image between bond points of 256×256 pixels within the categories of 2n pixels size, the good frequency plot results can be obtained. A 2D Fast Fourier Transform function transforms the spatial information of image into distribution of the points as shown in Fig. 22 (b);
2) an ImageJ oval plug-in was used to sum up pixel intensities along each radius from the origin of circle to the periphery; and
3) the total pixel intensity value was used to plot FFT alignment with normalization, shown in Fig. 22 (c).

Fig. 22 (c) shows that the peaks around 54 degrees, whereas majority of fibres align between 30- 80 degrees. This can be explained by the fact that lower portion of circumference is almost symmetric to the upper portion. This method is unable to give the accurate fibre alignment within the bond point of thermally bonded nonwoven fabric because the structure of thermally bonded nonwoven fabric is not in flat. Further future research will be required to analyse the 2D reconstructed stack sliced image of nonwoven fabric to give the exact fibre orientations. When exact fibre orientations are defined, the thermally anisotropic values of fibre can be provided to enabling higher value of effective thermal conductivity and closer to experimental result.

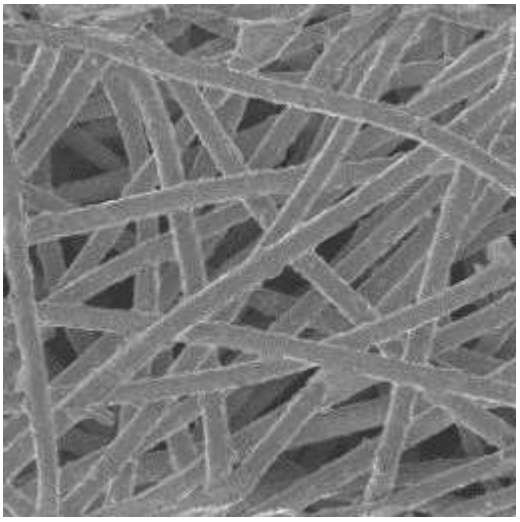

(a)

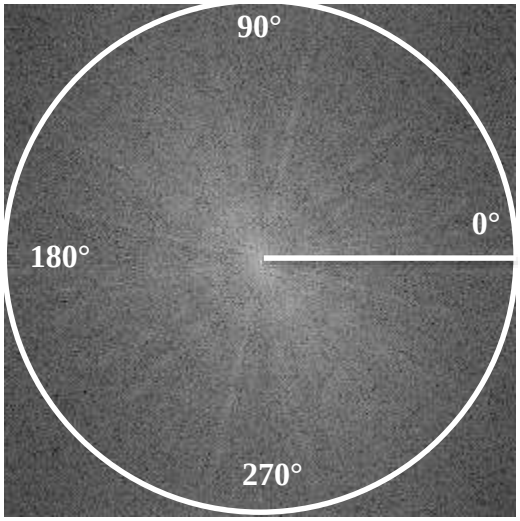

(b)

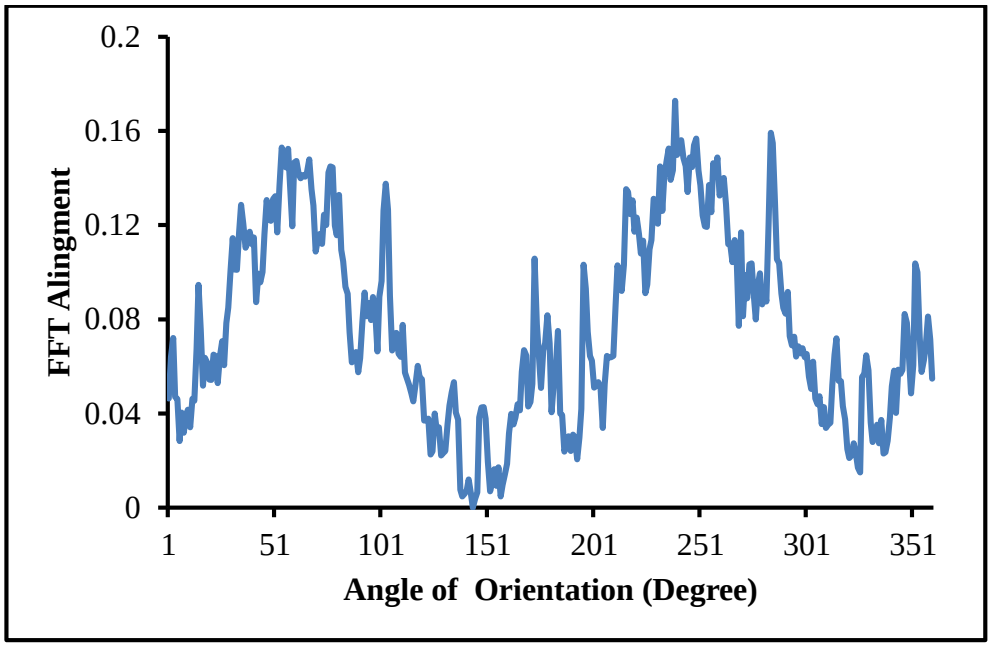

(c)

Fig. 22. Fibre orientation: (a) Grey scale cropped image of sample-1; (b) 2D FFT frequency plot of sample-1; and (c) 2D-FFT alignment plot of sample-1.

3.2 Predicted Results from Validated Models

The models was further analysed in order to evaluate some properties which cannot be experimentally tested. The effect of fibre volume fraction and fibre thermal conductivity on the effective thermal conductivity and thermal resistance of nonwoven fabric have been studied.

Fabric insulation values mainly depend on fibre volume fraction and thermal conductivity of fibre at constant fibre orientation. For this purpose the validated model of sample-1 was chosen to analyse the effect of fibre volume fraction and thermal conductivity of fibre on overall heat transfer.

Table VII and Fig. 23 show the effective thermal conductivity and thermal resistance of thermally bonded nonwoven at different levels of fibre volume fraction respectively. It can be clearly observed that the effective thermal conductivity increases with the increase of fibre volume fraction and it reverses in case of thermal resistance.

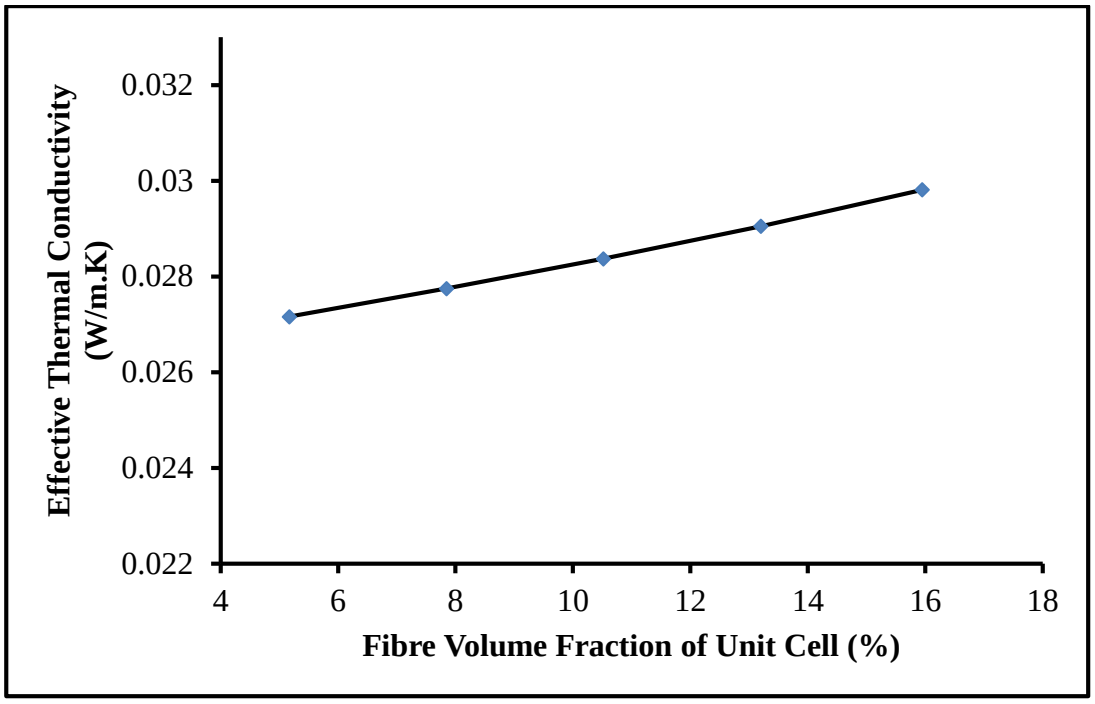

(a)

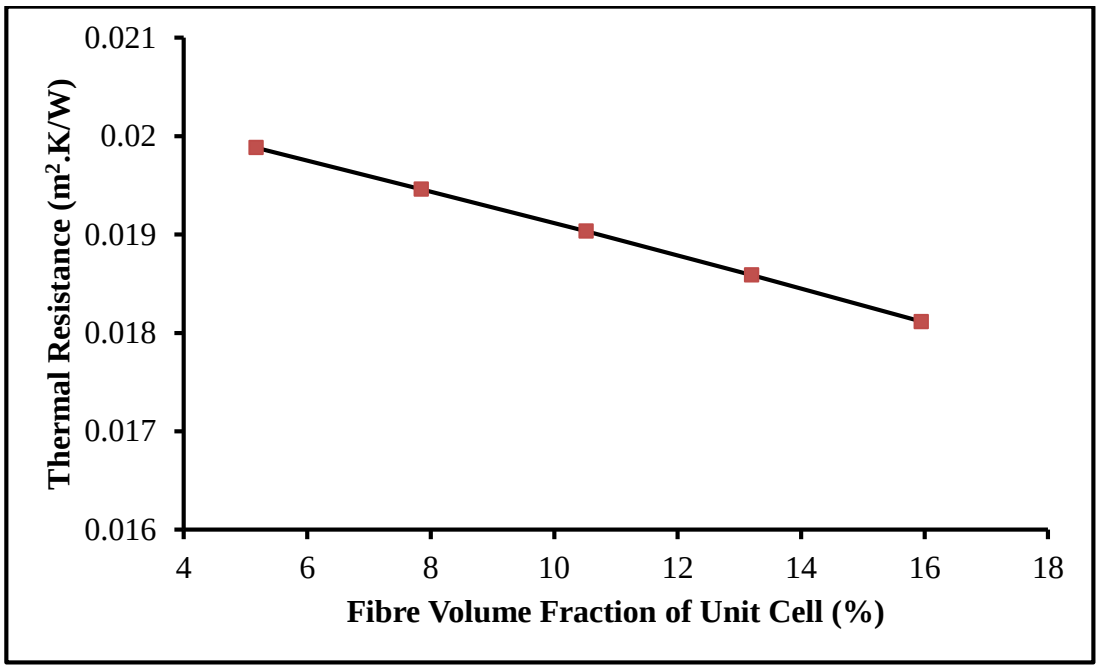

(b)

Fig. 23. (a) Relationship between fibre volume fraction and thermal conductivity of sample-1 nonwoven fabric and (b) Relationship between fibre volume fraction and thermal resistance of sample-1 nonwoven fabric.

Table VII: Effective thermal conductivity and thermal resistance at different fibre volume fraction

Fibre volume fraction of fibrous portion, V_{fp} (%)	Fibre Volume Fraction of unit cell, V_f (%)	Thermal Conductivity of fibrous portion, K_{fp} * (W/m.K)	Predicted effective thermal conductivity K_e (W/m.K)	Predicted thermal resistance R_e (m^2.K/W)
5.000	5.17	0.027035	0.02716	0.019882
10.00	7.85	0.028156	0.02775	0.019459
15.00	10.52	0.029374	0.02837	0.019034
20.00	13.20	0.030702	0.02905	0.018589
25.112	15.95	0.03219	0.02981	0.018115

* K_{fp} calculated on the bases of transverse thermal conductivity of fibre

The validated model of sample-1 was taken further to analyse the effect of fibre thermal conductivity on heat transfer phenomena. For this purpose a transient heat transfer analysis has been conducted by considering two different types of fibres polyester and polypropylene. Temperature specified boundary conditions were applied. At wall "A" 308.15 K was applied and the rest of the walls were considered as 298.15 K as shown in Fig. 24. It clearly shows that the temperature of the highlighted node in the fabric made of polyester fibre achieved temperature equilibrium faster than sample-1 made of polypropylene fibre. This agreed well with the fact that polyester fibre has higher thermal conductivity (0.157) than polypropylene fibre (0.11).

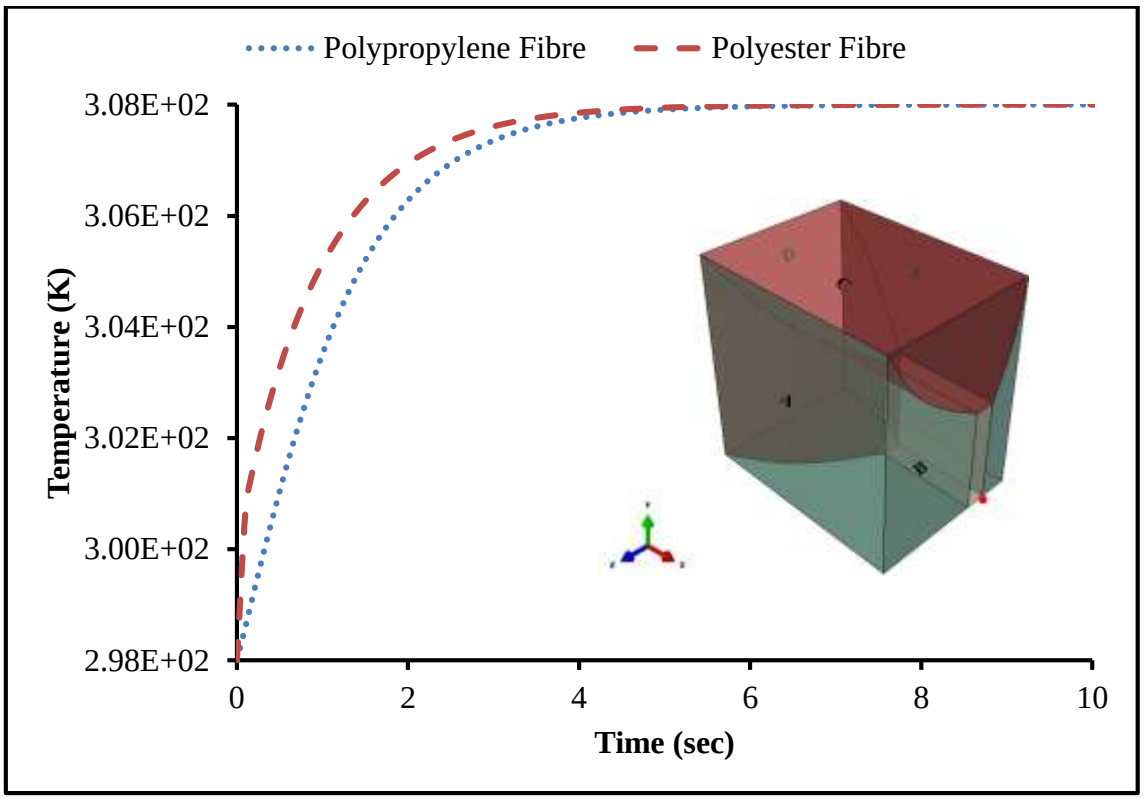

Fig. 24. Temperature profile of highlighted node of polypropylene and polyester sample-1.

4 Conclusions

Research techniques have been successfully developed to predict the effective thermal conductivity and thermal resistance of thermally bonded nonwoven fabrics by using two different unit cell models.

A good correlation coefficient and coefficient determination show the applicability of the developed techniques for the prediction of effective thermal conductivity and thermal resistance of thermally bonded nonwoven fabrics. Mean absolute error between experimental and predicted results shows that the thermal anisotropy and fibre orientation have significant influence on the effective thermal conductivity and thermal resistance of nonwoven fabrics and they should be considered for successful FE model development.

The validated models have been further used to study the effect of fibre volume fraction and thermal conductivity of fibre on the effective thermal conductivity and thermal resistance of thermally bonded nonwoven fabrics which cannot be directly tested through practice.

Acknowledgement

This research is financially supported by NED University of Engineering and Technology, Karachi, Pakistan.

References

1. EDANA. What are nonwovens?, http://www.edana.org/discover-nonwovens/what-are-nonwovens- (accessed 2015 28 February).
2. Bogaty H, Hollies NRS and Harris M. Some Thermal properties of fabrics: part I: The effect of fiber arrangement. *Textile Research Journal* 1957; 27: 445-449. DOI: 10.1177/004051755702700605.
3. Imakoma H, Sang H and Okazaki M. Effective thermal conductivity of fibrous insulations. *International chemical Engineering* 1990; 30: 738-746.
4. Naka S and Kamata Y. Thermal conductivity of wet fabrics *Journal of the Textile Machinery Society of Japan* 1976; 29: T114-T119.
5. Kawabata S. Measurement of anisotropic thermal conductivity of single fiber. *Journal of the Textile Machinery Society of Japan* 1986; 39: T184-T186.
6. Woo SS, Shalev I and Barker RL. Heat and moisture transfer through nonwoven fabrics: Part I: Heat transfer. *Textile Research Journal* 1994; 64: 149-162. DOI: 10.1177/004051759406400305.

7. Smith PA. Technical fabric structures – 3. Nonwoven fabrics. In: Horrocks AR and Anand SC (eds) *Handbook of technical textiles*. North and South America: Woodhead Publishing Limited, 2000, pp.130-151.
8. Zhu Q, Xie M, Yang J, et al. A fractal model for the coupled heat and mass transfer in porous fibrous media. *International Journal of Heat and Mass Transfer* 2011; 54: 1400-1409.
9. Zhu G, Kremenakova D, Wang Y, et al. An analysis of effective thermal conductivity of heterogeneous materials. *AUTEX Research Journal* 2014; 14: 14-21.
10. Venkataraman M, Mishra R, Jasikova D, et al. Thermodynamics of aerogel-treated nonwoven fabrics at subzero temperatures. *Journal of Industrial Textiles* 2015; 45: 387-404.
11. Zhang H, Hu J, Yang X, et al. Evaluation on Heat Transferring Performance of Fabric Heat Sink by Finite Element Modeling. *Journal of Textile Science and Technology* 2015; 1: 25.
12. Venkataraman M, Mishra R, Militky J, et al. Modelling and simulation of heat transfer by convection in aerogel treated nonwovens. *The Journal of The Textile Institute* 2017; 108: 1442-1453.
13. EDANA (2012), "EDANA 2012 nonwoven production statistics", http://www.edana.org/newsroom/news-announcements/news-article/2013/04/19/edana-2012-nonwoven-production-statistics (accessed July 2015).
14. Hearle JW and Morton WE. *Physical properties of textile fibres* 4th ed.: Woodhead, 2008.
15. Ostadi-Valiabad H. *Micro and nano scale three-dimensional reconstruction of polymer electrolyte fuel cell porous layers*. University of Birmingham, 2012.
16. ImageVis3D 3.0.0. NIH/NIGMS Center for Integrative Biomedical Computing (CIBC).
17. Rasband W. ImageJ. 1.48V ed. USA: National Institute of Helath, 2013.
18. Otsu N. A threshold selection method from gray-level histograms. *Systems, Man and Cybernetics, IEEE Transactions on* 1979; 9: 62-66. DOI: 10.1109/TSMC.1979.4310076.
19. Schmid B, Schindelin J, Cardona A, et al. A high-level 3D visualization API for Java and ImageJ. *BMC Bioinformatics* 2010; 11: 274.
20. Cignoni P. MesLab. 1.3.2 ed.: Visual Computing Lab-ISTI-CNR, 2012.
21. Siddiqui MOR and Sun D. Automated model generation of knitted fabric for thermal conductivity prediction using finite element analysis and its applications in composites. *Journal of Industrial Textiles* 2014. DOI: 10.1177/1528083714551440.

22. Ayres CE, Jha BS, Meredith H, et al. Measuring fiber alignment in electrospun scaffolds: a user's guide to the 2D fast Fourier transform approach. *Journal of Biomaterials Science, Polymer Edition* 2008; 19: 603-621. DOI: 10.1163/156856208784089643.